J Solid State Electrochem (2012) 16:911–919
DOI 10.1007/s10008-011-1441-5

ORIGINAL PAPER

Investigation on $LiCoPO_4$ powders as cathode materials annealed under different atmospheres

Lucangelo Dimesso · Susanne Jacke · Christina Spanheimer · Wolfram Jaegermann

Received: 28 February 2011 / Revised: 18 May 2011 / Accepted: 30 May 2011 / Published online: 11 June 2011

Abstract An uncomplicated Pechini-assisted sol–gel process in aqueous solutions is used for the synthesis of Li–Co phosphate powders as cathode materials. The powders are annealed under different conditions in flowing nitrogen and in flowing air. The structural, morphological, and electrochemical properties are strongly dependent upon the annealing conditions. After the treatment in air, the X-ray diffraction (XRD) patterns reveal the presence of $LiCoPO_4$ as a single phase. The morphology of the powders consists of a homogeneous and good interconnected blend of grains with different sizes; the cyclic voltammetry (CV) curves show a very good reversibility with very close values of the mean peak maxima in the cathodic region. The electrochemical measurements deliver a discharge specific capacity of 37 $mAhg^{-1}$ at a discharge rate of C/25 at room temperature. After annealing in nitrogen, the XRD analysis detects the formation of $Li_4P_2O_7$ and to Co_2P as secondary phases; the morphological investigation indicated that the $LiCoPO_4$ particles took shape of prisms with an average size of 2 μm. The CV curves are associated with a large polarization and poor irreversibility. The electrochemical measurements deliver a discharge specific capacity of 42 mAh g^{-1} at a discharge rate of C/25 at room temperature and lower capacity fade (approx. 35%).

Keywords Sol–gel · Cathode materials · Lithium cobalt phosphate · Annealing · Nitrogen · Air

L. Dimesso (✉) · S. Jacke · C. Spanheimer · W. Jaegermann
Materials Science Department,
Darmstadt University of Technology,
Petersenstrasse 32,
64287 Darmstadt, Germany
e-mail: ldimesso@surface.tu-darmstadt.de

Introduction

With the increasing demand for electric and hybrid electric vehicles to resolve energy and environmental problems, cathode materials with high specific energy density, high power density, and excellent thermal stability are necessary for Li-ion batteries (LIBs) [1]. The creation of redox-active transition metal framework structures that host mobile interstitial Li^+ ions is crucial in developing high-capacity LIBs. Lithium transition metal phosphates such as $LiFePO_4$ [2], $LiMnPO_4$ [3], $Li_3V_2(PO_4)_3$ [4, 5], and $LiVPO_4F$ [6, 7] have been recognized as promising positive electrodes for these systems because of their energy storage capacity combined with electrochemical and thermal stability. However, there are several problems with the use of metallophosphates as cathode materials, such as complex synthesis procedures, poor electronic conductivity, and low operating voltage, as extensively reported in literature.

Among the $LiMPO_4$ (M=Fe, Mn, Ni, and Co) family, Okada et al. [8] have shown that $LiCoPO_4$ has the highest redox potential. $LiCoPO_4$ is the only example of this class of materials that is suitable for 5-V performances. In fact, it can be considered as one of the best examples of 5-V cathode materials because of its high specific capacity and voltage. Studies on $LiCoPO_4$ (and $LiNiPO_4$) are scarce because the existing preferred non-aqueous electrolyte is found to be unstable in the high-voltage range (≥4.8 V) where cobalt and nickel reactions can occur. However, efforts toward improving non-aqueous electrolytes have made $LiCoPO_4$ an attractive cathode to explore in the high charge voltage regime, up to 5 V. Although the reversibility of ilthium extraction–insertion from/into $LiCoPO_4$ was demonstrated in a few reports [9–12], a severe capacity fading during cycling has limited the use of this material in practical applications. As result, less attention has been paid

toward the development of $LiCoPO_4$ cathode in lithium batteries using non-aqueous electrolytes.

$LiCoPO_4$ has been prepared using solid-state reactions [10–12] and soft chemistry routes [13–16]. The disadvantages of the solid-state processes are the absence of control of the microstructure, the overall agglomeration of the particles, contaminations due to possible reaction with the crucible, and lithium volatilization during a long heat treatment cycle.

The wet chemistry technique offering improvement in the terms of material preparation has been extensively used as a low-temperature synthesis route (T<200 °C). The numerous advantages of low-temperature methods including intrinsic ease of use, low cost, versatility in terms of composition and structure manipulations, and ease of various processing following synthesis make them especially appealing for preparing solid-state ionic materials. In fact, by using a simple sol–gel process, our group has successfully reported the preparation of $LiFePO_4$ powders as well as of $LiFePO_4$–carbon foam composites that have exhibited good performances as cathode materials [17, 18].

During the preparation process of the transition metals containing phosphates, the atmosphere plays an important role on the properties of the products such as phase formation, presence or not of secondary phases, morphology of the products, etc. While intensive investigations have been conducted on the effects of a reducing or strong reducing or inert atmospheres on the structure and on the surface properties of the $LiFePO_4$ as cathode material [19, 20], the authors have found a few literature references ([20] and references herein) dealing with the preparation of $LiCoPO_4$ powders via sol–gel process and annealed under reducing and oxidizing atmospheres.

In this study, the influence of thermal treatment under an inert atmosphere (flowing nitrogen) and under an oxidizing atmosphere (flowing air) on the structure, morphology, and electrochemical properties of $LiCoPO_4$ is investigated.

Experimental

The experimental procedures for the preparation and characterizations of the samples were similar to those reported earlier [17]. The $LiCoPO_4$ samples were prepared by dissolving in water $Li(CH_3COO)\cdot 2H_2O$ (lithium acetate), $Co(CH_3COO)_2\cdot 4H_2O$ (cobalt(II) acetate) as precursors (molar ratio 1:1) with citric acid (2 × mol [Co]), and then phosphoric acid in equimolar ratio with Li and Co ions was added. The starting solution, with a concentration of the precursors of 0.1 M, was slowly evaporated at 80 °C under air. After 3 h, a very homogeneous gel, containing Li, Co, and phosphate in the stoichiometric proportions of $LiCoPO_4$, is then produced. The homogeneous mixture was finally divided into two parts. The first part was progressively heat-treated in air at different temperatures, 300, 550, 750, and 800 °C, for 5 and 10 h (hereafter labeled as LCP-A), while the second part was treated under nitrogen at 300, 730, and 800 °C for 5 and 12 h, respectively (hereafter labeled as LCP-N).

The structural analysis of the samples was performed by X-ray powder diffraction using a D8 Bruker powder diffractometer (Cu $K\alpha_1$+Cu $K\alpha_2$ radiation) with a *theta/2 theta* Bragg–Bentano configuration. The diffractometer is equipped with an energy dispersion detector Si(Li) to minimize the fluorescence effects. A scanning electron microscope (Philips XL 30 FEG) was used to investigate the morphology of the samples. The X-ray-induced photoelectron spectroscopy (XPS) studies have been performed using a PHI 5700 spectrometer equipped with an Al-Kα (1,468.6 eV) source and a spectral resolution of <400 meV [21]. Electrochemical studies (e.g. cyclic voltammetry, CV) have been carried out with a multichannel potentiostatic–galvanostatic system VPM2 (Princeton Applied Research, USA). For the measurements, Swagelok-type cells were assembled in an argon-filled dry box with water and oxygen <5 ppm. The typical cathode material for the $LiCoPO_4$ powders annealed in nitrogen was fabricated as follows: 85 wt.% active material, 10 wt.% acetylene carbon black, and 5 wt.% PTFE (60 wt.% water dispersion, Aldrich) as binder were intimately mixed in a few milliliters of 2-propanol and treated in a ultrasound bath for 20 min at RT. The amount of the acetylene carbon black was raised up to 30 wt.% in the cathode compositions prepared with the $LiCoPO_4$ annealed in air. The resulting paste-like material was cut in pellets and dried out at 80 °C for 24 h under vacuum (resulting electrode containing 20–30 mg active compound). In the cell, Li metal was used as anode, SelectiLyte LF30 (1 M LiFAP in ethylene carbonate/dimethyl-carbonate 1:1 (*w*/*w*), Merck KGaA, Germany) as electrolyte [22–24], Celgard®2500 as separator. An aluminum foil was used as current collector. All electrical measurements were performed at room temperature.

Results and discussion

Structural analysis

The X-ray diffraction (XRD) patterns of the synthesized $LiCoPO_4$ powders treated in air at different temperatures for 5 h are shown in Fig. 1a–d. All the diffraction peaks have been indexed with the olivine-type symmetry (*Pnma*), which confirms that the structure of the prepared powders corresponds to the orthorhombic $LiCoPO_4$. The Bragg peaks of the samples measured after the calcinations revealed the poor crystalline nature of the material after

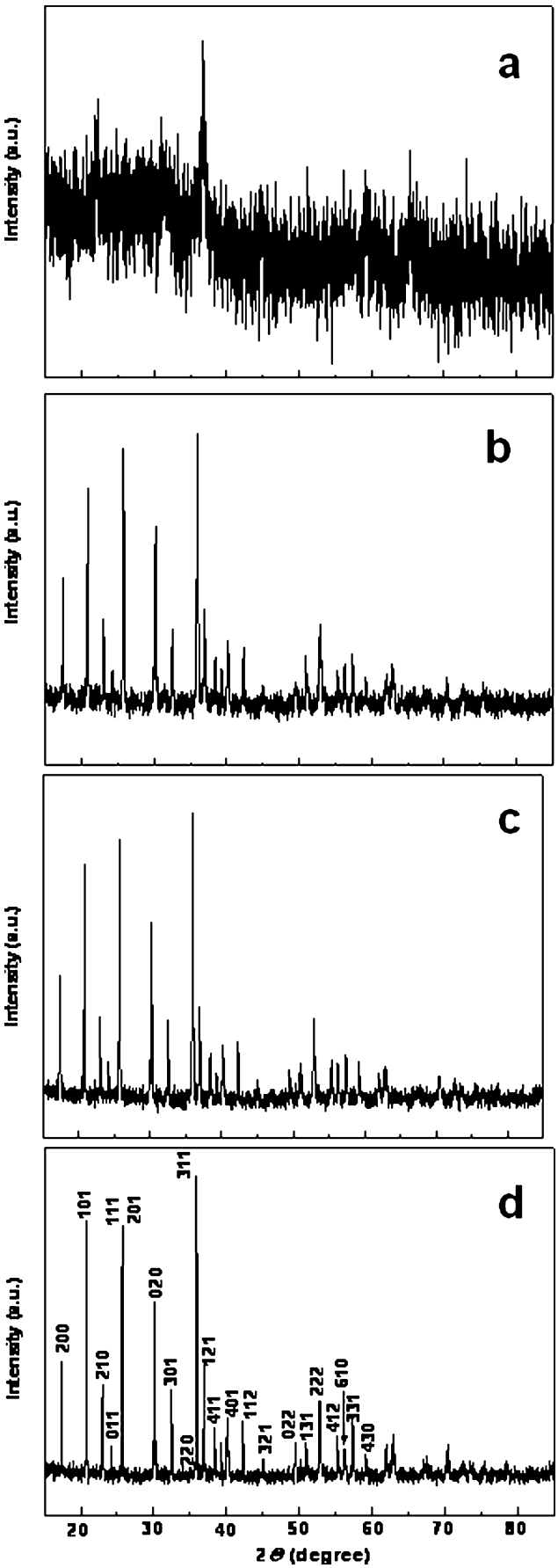

Fig. 1 X-ray diffraction patterns of the prepared $LiCoPO_4$ powders annealed in air for 5 h: at T=300 °C (**a**), at T=550 °C (**b**), at T=750 °C (**c**), and at T=800 °C (**d**), respectively

the treatment at lower temperature (≤300 °C, Fig. 1a). The formation of the $LiCoPO_4$ crystalline phase was observed after annealing at T=550 °C (Fig. 1b), confirming the data of Koleva et al. [25] who reported the growth of the $LiCoPO_4$ phase at 450 °C by preparing the cathode materials by freezing aqueous solutions of the corresponding metal formates and LiH_2PO_4. At higher annealing temperatures, the XRD diffractograms showed the growth of the $LiCoPO_4$ grains, as confirmed by the stronger and sharper crystalline reflections in Fig. 1c, d, respectively. In fact, the grain sizes of the samples, estimated using the Scherrer formula, were 45 nm for the powders annealed at 750 °C and 57 nm for the powders annealed at 800 °C.

The high thermal stability of the $LiCoPO_4$ olivine phase in air has been previously reported [13, 14, 26] and confirmed in this work by annealing the powders at 800 °C for 10 h. Comparing the XRD diffractograms of the at 800 °C annealed powders, the $LiCoPO_4$ phase was still detected as a single phase, and no parasitic phases have been observed after the annealing.

The XRD patterns of the synthesized $LiCoPO_4$ powders treated in nitrogen at different conditions are shown in Fig. 2a–c. The diffractograms confirmed the poor crystalline nature of the material after annealing at lower temperatures (≤300 °C, Fig. 2a). By annealing at temperatures ranging between 300 and 730 °C, the presence of $LiCoPO_4$ as a single crystalline phase has been detected (Fig. 2b). At higher annealing temperatures (T≥730 °C) and longer annealing time (t≥12 h), the XRD spectra showed the presence of crystalline reflections attributed to $Li_4P_2O_7$ and to Co_2P as secondary phases (indicated as (x) and (o), respectively, in Fig. 2c) [27]. The formation of such secondary phases, particularly of Co_2P, occurs due to the reduction at the grain boundaries of the $LiCoPO_4$ crystalline phase by heat treatment at high temperatures (≥700 °C). Whether the presence of these secondary phases leads to an improvement of the electrochemical performance of $LiCoPO_4$ is still under debate.

Scanning electron microscopy

The influence of the annealing atmosphere was also confirmed by the morphological investigation. A typical scanning electron microscopy (SEM) micrograph of the Co-containing phosphate after treatment in air is shown in Fig. 3a. After annealing at T=700 °C, the $LiCoPO_4$ powders appear as a homogeneous blend of grains with different sizes under 1.5 μm. Different morphological structures have not been detected, confirming the results

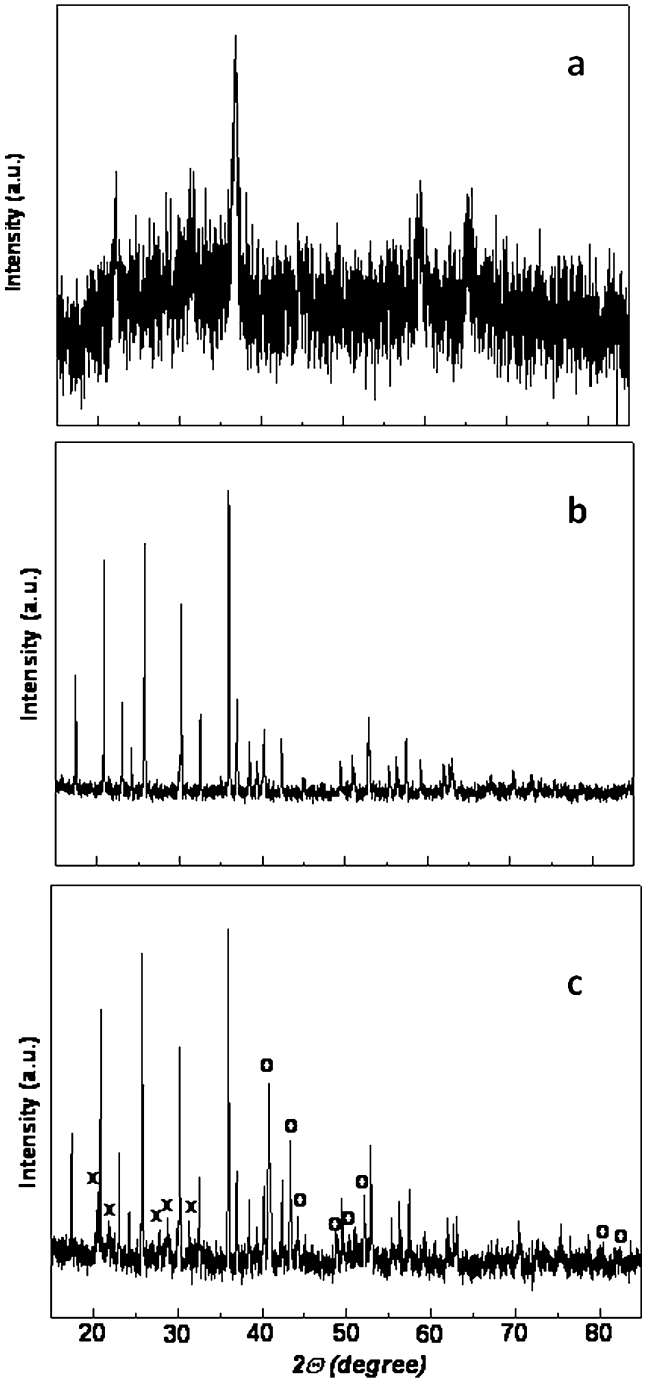

Fig. 2 X-ray diffraction patterns of the prepared $LiCoPO_4$ powders annealed in nitrogen for 5 h: at T=300 °C (**a**), at T=730 °C (**b**), and at T=800 °C (**c**), respectively. Secondary phases are indicated as *ex* for $Li_4P_2O_7$ and as *circles* for Co_2P

of the XRD analysis. By treating at higher temperatures (T=800 °C), the picture shows a better interconnected structure through the grain boundaries (Fig. 4a). The average grain size was estimated to range between 1 and 3 μm, confirming the data previously reported [15]. A similar morphology has been observed by Kim et al. [28], investigating $LiFePO_4$/Carbon composites prepared by polyol method. The authors claimed that particles with nanoplate-like shapes, a uniform size distribution, and an average grain size of 0.3 μm can improve the electrochemical performance of the cathode material by favoring lithium diffusion through the particles.

A different morphological behavior has been detected after annealing in nitrogen. The $LiCoPO_4$ powder is a mixture of polycrystalline particles with a very wide distribution range size, as one can observe in Fig. 3b. The morphology consists of aggregates of primary nanoparticles <500 nm in dimension partially embedded in a "matrix of amorphous carbon." The presence of the carbon on the surface is typically detected as residual using the Pechini (or Pechini-assisted) sol–gel process. The elemental analysis (CHNX analysis) revealed a content of amorphous carbon in the samples annealed in nitrogen of 9.5 wt.%. Furthermore, the obtained $LiCoPO_4$ particles took the shape of prisms with an average size of 2 μm, and the presence of secondary phases can be observed (Fig. 4b). A similar morphology has been reported by Huang et al. [29] by preparing the $LiCoPO_4$ phase under hydrothermal conditions; the authors explained the formation of $LiCoPO_4$ crystals through a "dissolution–crystallization" process.

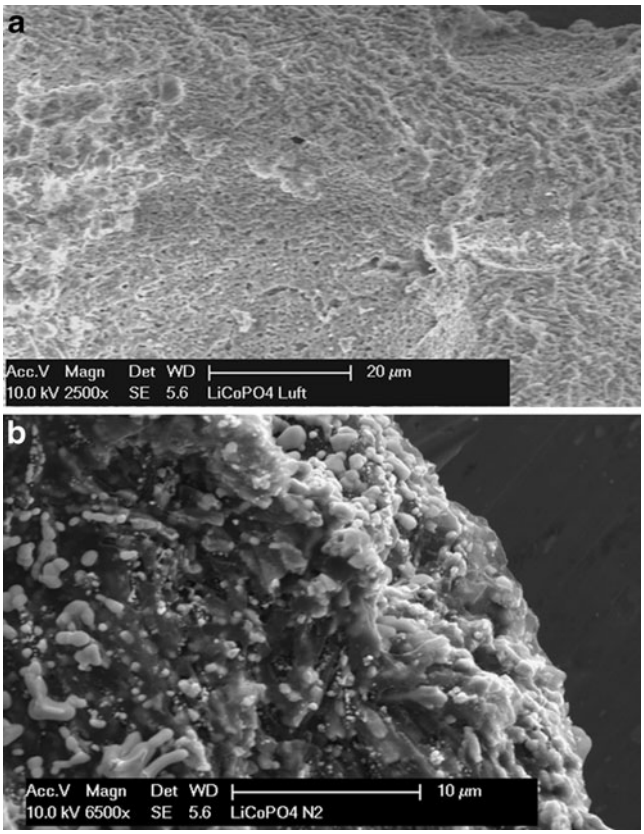

Fig. 3 SEM micrographs of the synthesized $LiCoPO_4$ powders after annealing for 5 h at: T=700 °C in air (**a**) and T=730 °C in nitrogen (**b**), respectively

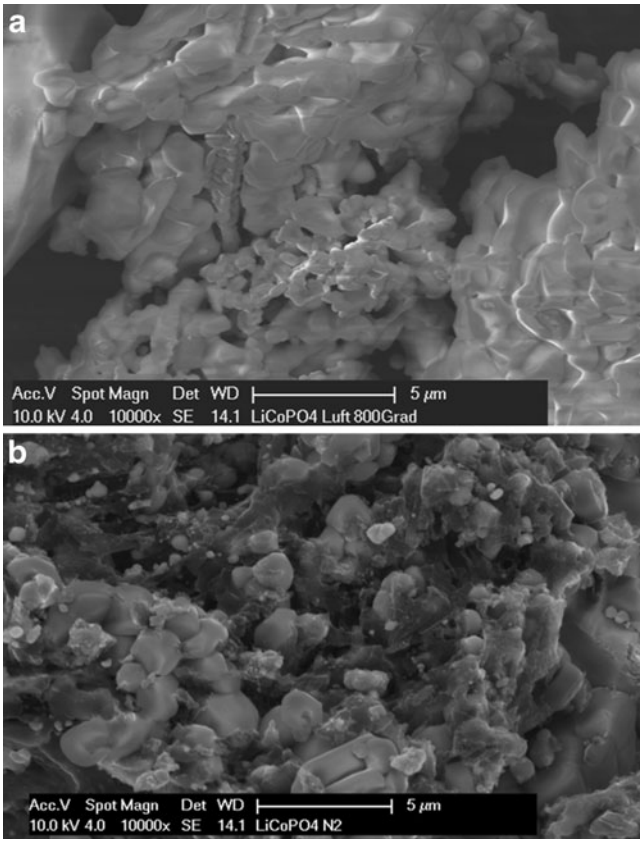

Fig. 4 SEM micrographs of the synthesized $LiCoPO_4$ powders after annealing at T=800 °C: in air for t=5 h (**a**) and in nitrogen for t=10 h (**b**), respectively

Under the hydrothermal conditions, the precursor of the Co (II) was partially dissolved because of the solubility at elevated temperatures. Therefore, the concentration of Co (II) was increased. At the same time, the solution trended to saturation for $LiCoPO_4$ due to the increase of Co(II) concentration and the alkalinity of the reaction medium. When a critical supersaturation of $LiCoPO_4$ was reached, the nucleation of the solid $LiCoPO_4$ took place.

Under the experimental conditions of our work, a very similar "dissolution–recrystallization" process may have taken place. Independently of the process mechanism, the morphological investigation confirmed the reduction of the Co-containing olivine phosphates, leading to the formation of crystallites of metal phosphides (in this case Co_2P).

XPS analysis

XPS core-level analysis has been carried out on air-annealed and nitrogen-annealed powders. Although the XPS spectra of the samples annealed in air showed the typical shape of the XPS spectra reported in the literature for the corresponding oxidation state of the investigated ions, the XPS high-resolution spectra Co2p, O1s, P2p, Li1s, and C1s respectively showed shifts of the energy bindings (EBs) to higher values (approx. +8 eV) due to a "charge-induced shifting" effect [30]. This effect is well known for non-conductive (insulating) materials or conductors that have been deliberately insulated from the sample mount. The shift toward higher values of EBs is normally due to a shortage of electrons within the top 1–12 nm of the material surface caused by the loss of photo-emitted electrons. The degree of charging depends upon several factors such as the physical and chemical properties of the material (size, composition, homogeneity) as well as the technical parameters of the spectrophotometer (geometry, mounting technique of the sample on the sample holder). The XPS measurements in combination with the results of the XRD patterns can confirm the successful synthesis of the $LiCoPO_4$ phase after annealing in air.

The high-resolution Co2p spectrum of the samples annealed in nitrogen is very similar to those reported by Tan et al. [31] with a binding energy peak at 781.9 eV. The P2p binding energy is located at 133.7 eV, while the high-resolution C1s spectrum (Fig. 5) shows the carbon peak at 284.5 eV and is asymmetric in nature. A very small shoulder (reaching a value of EB of 287 eV) may indicate the presence of a very small amount of C–N group with some carbon–oxygen groups. From the presence of carbon, phosphor, and cobalt, we can reasonably assume the formation of a Co–P–C phase, which gives rise to the formation of cobalt phosphide and Li–P–O phase as by-products during the cooling step of the process [32].

Electrochemical measurements

Unlike the $LiFePO_4$, the electrochemical activity of the $LiCoPO_4$ system is still a controversial debate and has not been fully understood.

Extensive investigations on the electrochemical properties of the Li_xCoPO_4 system prepared by the sol–gel process have been recently reported ([32, 33] and references herein). The authors observed the presence of two plateaus in the charge curve (corresponding to $0.7 \leq x \leq 1.0$ and $0 \leq x \leq 0.7$, respectively, in the stoichiometric compound) independently of the electrolyte used during the measurements, which supports the idea that two-step delithiation is an intrinsic property of the system. This model was supported using in situ and ex situ XRD to explain the Li extraction/insertion mechanism in $LiCoPO_4$. However, the XRD results showed that the crystalline phase was only a lithium-poor phase; no "$CoPO_4$" was identified even though $LiCoPO_4$ was fully charged [32].

Our investigation showed the influence of the structural and morphological properties, that is to say, of the annealing conditions on the electrochemical performance of the $LiCoPO_4$ system.

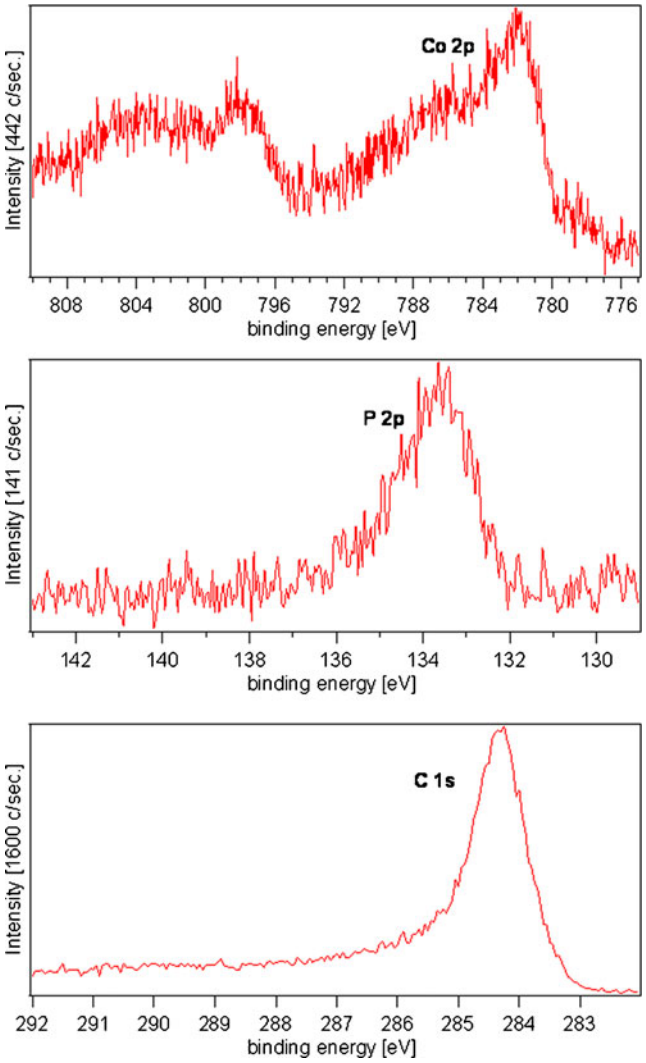

Fig. 5 XPS spectra in the region of Co2p, P2p, and C1s for $LiCoPO_4$ powders annealed in nitrogen at T=730 °C for t=5 h

Cyclic voltammograms (CVs) for $LiCoPO_4$ powders using Li metal as the counter and reference electrode cycled in the range 3.0–4.9 V for the samples annealed in air and in the range 3.0–5.0 V for the samples annealed in nitrogen are shown in Fig. 6a, b, respectively. The deintercalation/intercalation potentials corresponding to the mean peak maxima for all the samples are shown in Table 1. The CV curves show that the shape of the first cycle is quite different, as also revealed by the events at 3.58 V (reported in [15] as well) and 4.77 V, respectively, during the anodic process, while CV profiles are almost reduplicate from the second cycle, as revealed by the very close values of the mean peak maxima in the cathodic region. This is possibly due to a structural rearrangement in $LiCoPO_4$ taking place during the first charge process of the $LiCoPO_4$ powders. The asymmetry between the cathodic and anodic CV plots could imply that the Li-ion diffusion in $LiCoPO_4$ powders obeys a different mechanism between the charge and discharge processes, as proven out recently by Xie et al. [33] by measuring the Li-ion chemical diffusion coefficients on thin films prepared by rf magnetron sputtering.

On the other side, the CV curves of the samples annealed under nitrogen were associated with a large polarization and poor irreversibility. In our case, the reduction peak maximum can be barely determined after the third cycle. An explanation of this poor performance can be attributed to the presence of a rigid surface layer. In our case, Co_2P displays considerable hardness along with high electronic conductivity, and this means that additional energy may be required for the egress and ingress of lithium through the compact layer within the first few charge and discharge processes. During the cycling, the electrochemical kinetics can be strongly inhibited and high polarization overpotential is present.

The charge and discharge curves (voltage range between 3.0 and 5.3 V) as a function of the time and the voltage–capacity curves for the first and second charging for

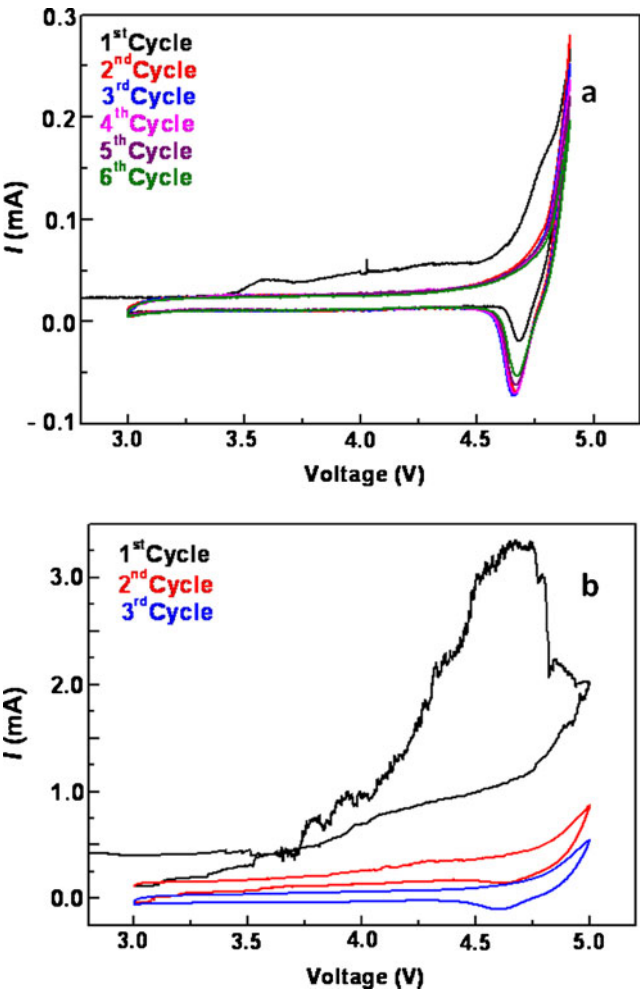

Fig. 6 Cyclic voltammograms recorded for the $LiCoPO_4$ composites after annealing: in air at T=800 °C for t=5 h (**a**) and in nitrogen at T=730 °C for t=12 h (scan rate, 0.05 mV s^{-1}, in the potential range 2.5–5.0 V vs. Li^+/Li) (**b**)

Table 1 Values of the deintercalation/intercalation potentials (peak maxima in Fig. 6a, b) for $LiCoPO_4$ powders after annealing under different atmospheres

Annealing conditions (atmosphere, T (°C), time (h))	Cycle (n)	Deintercalation potential (V)	Intercalation potential (V)
Air, 800, 12	1	3.58(?), 4.77	4.68
	2–6	–	4.65–4.67
Nitrogen, 730, 12	1	–	–
	2	–	4.63
	3	–	4.60

$LiCoPO_4$ powders annealed in air at T=800 °C for t=12 h (ACB, 30 wt.%) are shown in Fig. 7a, b. The cycling curves as a function of time, shown in Fig. 7a, are very similar to those reported by Bramnik et al. [34]. The researchers charged the cell galvanostatically by applying a current pulse until 5.0 V (at a discharging rate of C/3), then recorded the open-circuit voltage and the impedance spectra during the relaxation periods before and after charging. The researchers detected the existence of two plateaus during relaxation, which could be an indication of a self-discharge proceeding leading to the formation of the pristine compound, from which lithium can be extracted again. In fact, charging the cell again after the relaxation period revealed the two plateaus in the charge curve that are characteristic for $LiCoPO_4$. In the potential range 5.0–5.3 V (blue arrow in Fig. 7a), our measurements confirm the coexistence of "lithiated" and (partially or totally) "delithiated" phases. In fact, the voltage–capacity curves for the first and second charging processes (reported in Fig. 7b) have very similar shapes to those reported by Castro et al. [35] and Dahn et al. [36] concerning the $LiFePO_4/FePO_4$ system. By measuring the Fe2p XPS core peaks of the starting $LiFePO_4$-positive electrode, after the first electrochemical charge and after discharge, Castro et al. [35] confirmed that Fe is almost totally at the +III oxidation state at the end of the charge (i.e., when lithium has been deintercalated). Only a weak shoulder shows that a weak proportion of Fe^{2+} still remains in the material. At the end of the first cycle (discharge), the authors observed that the Fe2p spectrum was very close to that of the starting electrode, which showed that the +II oxidation state of iron has been recovered and confirmed the reversibility of the lithium extraction/insertion mechanism in the material.

The powders were also prepared into electrodes and cycled at different C rates ranging from C/25 to C/2. According to our data, the annealing atmosphere plays an important role on the specific capacity during the charging/discharging processes of the $LiCoPO_4$ system. As an example, the specific capacity of the $LiCoPO_4$ phase, measured at a discharge rate of C/25 and RT, after annealing in air and nitrogen is shown in Fig. 8. After annealing in air, at the end of the first cycle, the specific capacity is 37 mAh g^{-1}, while this value decreases rapidly and is only 15 mAh g^{-1} after the tenth cycle. At higher discharge rates, the specific capacity of $LiCoPO_4$ decreases dramatically, reaching barely 5 mAh g^{-1} at a discharge rate of C/5. Although the reversibility of lithium extraction–insertion from/into $LiCOPO_4$ was demonstrated in a few reports [10, 11], a severe capacity fading during cycling has limited the use of this material in practical application. Poor electronic conductivity is another common problem which hampers olivine-type materials. As mentioned before, the structural and morphological investigations and the elemental chemical analysis revealed no traces of secondary phases responsible for the capacity fading of the material. The absence of electron-conducting phases and the possible lack of lithium ions due to the long treatment at high temperature could reasonably lead to a faster formation of

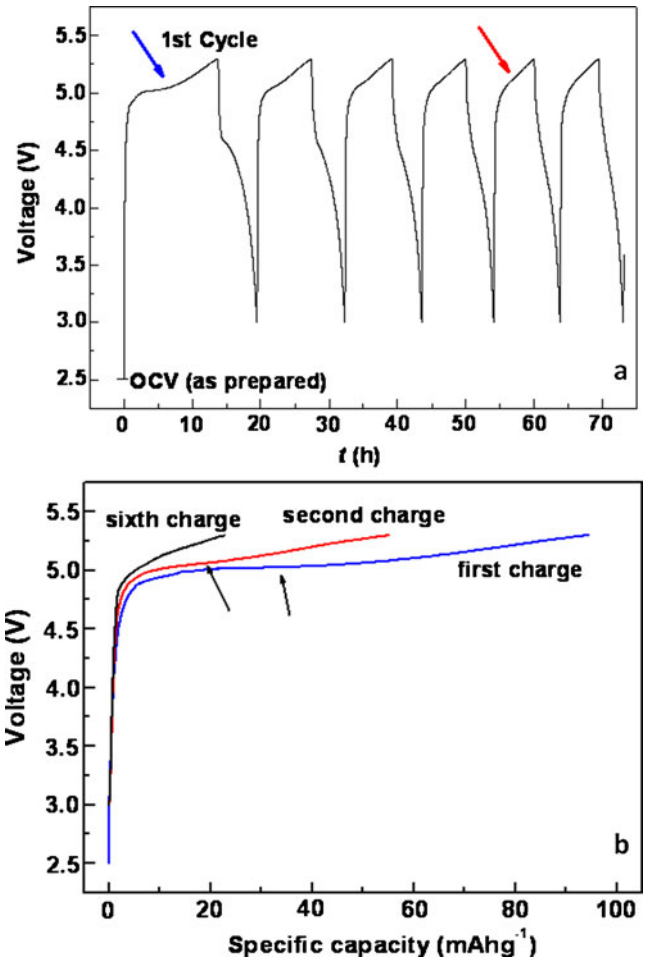

Fig. 7 **a** Charge and discharge curves (range, 3.0–5.3 V) as a function of time. **b** Voltage–capacity curves for the first, second, and sixth charging measured at the C/25 discharge rate and room temperature for $LiCoPO_4$ powders annealed in air at T=800 °C for t=12 h (ACB, 30 wt.%)

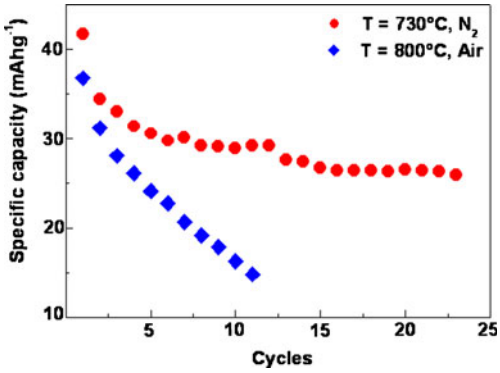

Fig. 8 Discharge capacity for $LiCoPO_4$ powders measured at a discharge rate of C/25 and RT, annealed for t=12 h under air at T=800 °C and under nitrogen at T=730 °C, respectively

the $CoPO_4$ phase during the delithiation process. $CoPO_4$ is unstable at room temperature, and sufficient quantities of this material, which often becomes non-crystalline, lead to a quick fade in capacity [13, 30].

On the other side, after annealing under nitrogen, at the end of the first cycle, the specific capacity reaches 42 mAh g^{-1}, while this value decreases slower and becomes stable (27 mAh g^{-1}) after the 15th cycle. The lower capacity fading can be explained by the electronic conduction due to the presence of elemental carbon in the material as well as by the presence of the cobalt phosphides on the surface which work as a "shield" against (or slow down) the amorphization of $CoPO_4$.

The electrolytes play a very important role in the electrochemical measurements that the thermodynamic instability of the electrolyte at the operation voltage close to 5 V vs. metallic lithium could be the reason for the drastic capacity losses as well. If a side reaction upon charging of the cell occurs, it contributes to the charge passed through the cell and then biases the calculation of the amount of extracted lithium. On the other hand, the degradation of the electrolyte on the cathode side may cause a limitation in mass transport on the cathode/electrolyte interface.

The use of a new salt (LiFAP–$LiPF_3(CF_2CF_3)_3$) ([23, 24] and references herein) with relatively stable P–F bonds has improved the quality of our work and allowed opening a new way to better understand the electrochemical behavior of the $LiCoPO_4$ compound. Further investigations are necessary in order to better understand their chemical, physical, and electrochemical properties to meet the requirements for industrial applications.

Conclusions

The influence of the annealing atmosphere on the structural, morphological, and electrochemical properties of the $LiCoPO_4$ system has been investigated.

The X-ray diffraction patterns of the prepared powders after annealing in air confirmed the presence of $LiCoPO_4$ with an olivine-like structure as a single phase. After treatment in nitrogen, the XRD analysis confirmed the presence of $LiCoPO_4$ as a single crystalline phase after annealing at T=730 °C for t=5 h only. For longer annealing time (t=12 h), the spectra showed the presence of crystalline reflections due to $Li_4P_2O_7$ and to Co_2P, respectively.

The morphological investigation of $LiCoPO_4$ powders after annealing in air revealed a homogeneous blend of grains with different sizes under 1.5 μm. Different morphological structures have not been detected, confirming the results of the XRD analysis. The homogeneous structure becomes better interconnected after annealing at higher temperature. After annealing in nitrogen, the $LiCoPO_4$ morphology consists of a mixture of polycrystalline particles with a very wide distribution range size. At higher annealing temperatures, the obtained $LiCoPO_4$ particles took the shape of prisms with an average size of 2 μm.

The XPS high-resolution spectra Co2p, O1s, P2p, and Li1s, respectively, of the samples annealed in air showed shifts of the EBs to higher values due to a "charge-induced shifting" effect, which is well known for non-conductive (insulating) materials. The presence of carbon was detected as well as the typical residual of the sol–gel process.

After annealing in air, the CV curves show that the shape of the first cycle is quite different, while the CV profiles are almost reduplicated from the second cycle, as revealed by the very close values of the mean peak maxima in the cathodic region. This is possibly due to a structural rearrangement in $LiCoPO_4$ taking place during the first charge process of the $LiCoPO_4$ powders. The CV curves for the $LiCoPO_4$ powders annealed under nitrogen were associated with a large polarization and poor irreversibility. The reduction peak maximum can be barely determined after the third cycle.

The powders were also prepared into electrodes and cycled at different C rates ranging from C/25 to C/2. After annealing in air, at the end of the first cycle, the specific capacity is 37 mAh g^{-1}, while this value decreases rapidly and is only 15 mAh g^{-1} after the tenth cycle. At higher discharge rates, the specific capacity of $LiCoPO_4$ decreases dramatically, reaching barely 5 mAh g^{-1} at a discharge rate of C/5. The absence of electron-conducting phases and the possible lack of lithium ions due to the long treatment at high temperature could reasonably lead to the fast formation of the $CoPO_4$ phase during the delithiation process. After annealing under nitrogen, at the end of the first cycle, the specific capacity reaches 42 mAh g^{-1}, while this value decreases slower and becomes stable (27 mAh g^{-1}) after the 15th cycle (65% of the initial value). The lower capacity fading can be explained by the electronic conduction due to

the presence of elemental carbon into the material as well as by the presence of the cobalt phosphides on the surface which work as a "shield" against (or slow down) the amorphization of $CoPO_4$.

Acknowledgments Many thanks are owed to Mr. J.-C. Jaud for the technical assistance in the XRD analysis. The authors thank the *Deutsche Forschungsgemeinschaft* (DFG) (*Sonderinitiativeproject: PAK-177*) for the financial support during this work. The DFG encourage and financially support the publication of the results during the projects. The DFG have no involvement in the study design, in analysis and interpretation of data, in the writing of the report, and in the decision to submit the paper for publication.

References

1. Han DW, Kang YM, Yin RZ, Song MS, Kwon HS (2009) Electrochem Commun 11:137–140
2. Pahdi AK, Nanjundaswami KS, Goodenough JB (1997) J Electrochem Soc 144:1188
3. Li G, Azuma H, Tohda M (2002) Electrochem Solid-State Lett 5:A135
4. Huang H, Yin SC, Kerr T, Nazar LF (2002) Adv Mater 14:1525
5. Yin SC, Strobel P, Anne M, Nazar LF (2003) J Am Chem Soc 125:10402
6. Barker J, Saidi MY, Swoyer JL (2002) US Patent 6,387,568
7. Barker J, Saidi MY, Swoyer JL (2003) Electrochem Solid-State Lett 6:A1
8. Okada S, Sawa S, Egashira M, Yamaki J, Tabuchi M, Kageyama H, Konishi T, Yoshio A (2001) J Power Sources 97:98–430
9. Nakayama M, Goto S, Uchimoto Y, Wakihara M, Kitajima Y (2004) Chem Mater 16:3399
10. Amine K, Yasuda H, Yamachi M (2000) Electrochem Solid-State Lett 3:178–179
11. Loris JM, Pèrez Vicente C, Tirado JL (2002) Electrochem Solid-State Lett 5:A234–A237
12. Jin B, Gu HB, Kim KW (2008) J Solid-State Electrochem 12:105–111
13. Bramnik NN, Nikolowski K, Trots DM, Ehrenberg H (2008) Electrochem Solid-State Lett 11(6):A89–A93
14. Gangulibabu, Bhuvaneswari D, Kalaiselvi N, Jayaprakash N, Periasamy P (2009) J Sol–Gel Sci Technol 49:137–144
15. Bhuwaneswari MS, Dimesso L, Jaegermann W (2010) J Sol–Gel Sci Technol 56:320–326
16. Vasanthi R, Kalpana D, Renganathan NG (2008) J Solid-State Electrochem 12:961–969
17. Dimesso L, Spanheimer C, Jacke S, Jaegermann W (2011) J Power Sources 196:6729–6734
18. Dimesso L, Jacke S, Spanheimer C, Jaegermann W (2011) J Alloys Comps 509:3777–3782
19. Zaghib K, Charest P, Guerfi A, Shim J, Perrier M, Kiebel K (2004) J Power Sources 134:124
20. Rho YH, Kanamura K, Fujisaki M, Hamagami J, Suda S, Umegaki T (2002) Solid State Ionics 151(1–4):151–157
21. Thissen A, Ensling D, Liberatore M, Wu QH, Fernandez Madrigal FJ, Bhuvaneswari MS, Hunger R, Jaegermann W (2009) Ionics 15:393–403
22. Merck. http://www.merck-chemicals.com. Accessed 31 January 2010
23. Schmidt M, Heider U, Kuehner K, Oesten R, Jungnitz M, Ignatev N, Sartori P (2001) J Power Sources 97–98:557
24. Gnanaraj JS, Zinigrad E, Levi MD, Aurbach D, Schmidt M (2003) J Power Sources 119–121:799–804
25. Koleva V, Zhecheva E, Stoyanova R (2010) Eur J Inorg Chem 2010:4091–4099
26. Saint-Martin R (2008) Franger S J Crystal Growth 310:861–864
27. Ellis B, Herle Subramanya P, Rho YH, Nazar LF, Dunlap R, Perry LK, Ryan DH (2007) Faraday Discuss 134:119–141
28. Kim DH, Kim TR, Im JS, Kang JW, Kim J (2007) J Phys Scr T129:31
29. Huang X, Ma J, Wu P, Hu Y, Dai Z, Zhu Z, Chen H, Wang H (2005) Mater Lett 59:578–582
30. Ehrenberg H, Bramnik NN, Senyshyn A, Fuess H (2009) Solid State Sciences 11:18–23
31. Tan L, Luo Z, Liu H, Yu Y (2010) J Alloys Comps 502:407–410
32. Rho YH, Nazar LF, Perry L, Ryan D (2007) J Electrochem Soc 154(4):A283–A289
33. Xie J, Imanishi N, Zhang T, Hirano A, Takeda Y, Yamamoto O (2009) J Power Sources 192:689–692
34. Bramnik NN, Nikolowski K, Baehtz C, Bramnik KG, Ehrenberg H (2007) Chem Mater 19:908–915
35. Castro L, Dedryvère R, El Khalifi M, Lippens P, Bréger J, Tessier C, Gonbeau D (2010) J Phys Chem 114:17995–18000
36. Dahn J, Jiang J, Moshurchak L, Buhrmester C, Wang RL (2005) Electrochem Soc Interface 14(4):27–31